Antigenic strain diversity explains different biogeographic patterns of invasion and maintenance of anti-malarial drug resistance

Qixin He[1◑*], John K. Chaillet[1◑], Frédéric Labbé[2,3]

1 Department of Biological Sciences, Purdue University, West Lafayette, IN, USA
2 Department of Ecology and Evolution, University of Chicago, Chicago, IL, USA
3 CIRAD, UMR PVBMT, F-97410 Saint Pierre, La Réunion, France

◑These authors contributed equally to this work.
* heqixin@purdue.edu

Abstract

The evolution of drug resistance in malaria poses a significant challenge to effective treatment and intervention efforts. Despite extensive investigation, no consensus has been reached on the relationship between transmission intensity and drug resistance. This may be due to the lack of consideration of antigenic diversity and its interaction with host immunity and multiplicity of infection. To better understand different biogeographic patterns of drug resistance evolution, we developed a novel compartmental model based on a macroparasite modeling approach that explicitly tracks the population sizes of sensitive and resistant parasite strains, host populations with different levels of generalized immunity, and their infection histories. Particularly, in this model, strain-specific immunity toward surface proteins determines the success probability of new infections, while generalized immunity of the hosts determines the likelihood of clinical symptoms that modulate drug usage. Our results demonstrate a negative correlation between parasite prevalence and resistant frequency, irrespective of resistance cost. We validate this general trend by analyzing data from studies reporting the frequency of chloroquine-resistant markers before the usage ban. Furthermore, the model accurately predicts the divergent biogeographic responses after drug discontinuation: resistant genotypes are maintained at high frequencies in low-diversity low-transmission regions, whereas in high-diversity high-transmission regions, the frequency of resistance undergoes a steady decrease. Our results highlight the crucial role of malaria strain diversity in the biogeographic patterns of resistance evolution.

Introduction

Prolonged usage of antimicrobial drugs almost always results in the emergence and spread of resistant strains [1]. The history of falciparum malaria chemotherapy over the last hundred years witnessed a succession of five classes of drugs region by region as resistant strains established to an alarming frequency [2]. However, the patterns of drug resistance evolution, such as the speed of establishment and equilibrium frequencies, differ drastically across different biogeographic regions. Even though *de novo* resistant alleles are constantly generated, widespread resistant strains can almost always be traced back to two unstable tranmission regions, i.e., Southeast Asia (especially the Greater Mekong Subregion) and South America [3–5]. While the frequencies of resistant

genotypes often sweep close to fixation in these regions [6, 7], their frequencies are more variable in endemic transmission regions such as sub-Saharan Africa [8]. More interestingly, while in high-transmission regions, a steady decrease of resistant genotypes often ensues from reducing the particular drug usage [9, 10], resistant genotypes are maintained at high frequency in low or unstable transmission regions even after the abandonment of the drug for several decades [11].

Plenty of mathematical models have been developed to explain some but not all of the empirical drug-resistance patterns. Various relationships between transmission intensity and stable frequencies of resistance were discovered, each of which has some empirical support: 1) transmission intensity does not influence the fate of resistant genotypes (Model: [12]; Empirical: [13–15]; 2) resistance increases in frequency and slowly decreases with increasing transmission rates (Models: [16, 17]); and 3) Valley phenomenon: resistance can be fixed at both high and low end of transmission intensity (Model: [18]; Empirical: [8]). In other stochastic models, resistance is found to be harder to spread under high transmission regions, but patterns are not systematically inspected across the parameter ranges (Model: [19]; Model and examples in [20]); Under non-equilibrium scenarios, i.e., where insecticides or bednets temporarily reduced transmission, reductions in resistance frequency were also observed [21–23]. Varying predictions of the relationships can be attributed to three model assumptions: 1) whether and how population immunity is considered, 2) how the cost of resistance is modeled, and 3) whether and how multiplicity of infection (MOI) is included. It is, therefore, critical to formulate a generalizable mathematical model that captures the most important biological processes that directly impact the survival and transmission of the parasites.

While most models have explored factors such as drug usage [12, 17], vectorial capacity [18, 24], within-host competition [24, 25], population immunity [16, 18], and recombination [26–29], strain diversity of parasites has not been explicitly considered in mathematical models of drug resistance. Yet, orders of magnitude differentiate antigenic diversity of *Plasmodium faciparum* strains among biogeographic zones and drive key differences in epidemiological features [30, 31]. Hyper-diverse antigens of parasites in sub-Saharan Africa emerged from the long-term co-evolutionary arms race among hosts, vectors, and parasites [32]. In endemic regions of falciparum malaria, hosts do not develop sterile immunity and can constantly get reinfected with reduced symptoms [33]. These asymptomatic carriers of the parasite still constitute part of the transmission and serve as a reservoir of strain diversity [34, 35] despite the fact that parasite prevalence decreases with host age in endemic regions [36]. This age-prevalence pattern was attributed to acquired immunity after repeated infections and represented as different generalized immunity classes in disease dynamics models [16, 37, 38]. Recent advances in molecular epidemiology indicate the importance of strain-specific immunity [39].

During the asexual blood stage, intra-erythrocytic parasites express adhesin proteins at the red blood cell surface that help mediate binding to the epithelial layers of vasculature to avoid the clearance by spleen during circulation [40]. One of the major surface proteins, *P. falciparum* erythrocyte membrane protein 1 (PfEMP1), is encoded by *var* genes, a gene family of $\tilde{6}0$ different copies within a single parasite genome [41]. Immune selection maintains the composition of *var* genes between different strains with minimal overlap [42]. In high endemic regions, many antigenically distinct strains (or modules of strains) coexist in the transmission dynamics [43]. Whether the hosts have seen the specific variants of the *var* genes largely determines the clearance rate of the parasites [44, 45]. Therefore, host-specific immunity, acquired from exposure to local antigenic diversity, plays a key role in local transmission dynamics as well as the fate of resistance. Thus, under the same vectorial capacity, different strain diversity results in significant changes in population-level immunity and transmission intensity, and the

ensuing epidemiological patterns, such as multiplicity of infection (MOI), age-prevalence curve, and the ratio of asymptomatic infections [34, 46]. These changes, in turn, alter the fate of resistance invasion. Therefore, in addition to generalized immunity represented in earlier studies, models need to formally incorporate specific immunity.

Another challenging aspect for earlier models is whether and how multiclonal infections (those with MOI> 1) are considered. Due to malaria's long duration of infection [47], it is common for the host to carry infections that are contracted from separate bites, referred to as superinfections. Meanwhile, hosts can also receive multiple genetically distinct strains from a single bite, especially in high-transmission endemic regions [48–50]. Susceptible-Infected-Recovered (SIR) Models that only consider non-overlapping infections [12, 16, 18] cannot incorporate within-host dynamics of strains explicitly, which strongly impacts the fitness of resistant genotypes [51, 52]. Other superinfection models employ complex structures or specific assumptions that make it hard to link MOI with strain diversity or host immunity [12, 17].

Here we present a novel Ordinary Differential Equations (ODE) model that represents how strain diversity and vectorial capacity influence transmission intensity, hosts' strain-specific and generalized immunity, and the resulting MOI distribution. In this model, strain-specific immunity toward diverse surface proteins determines the probability of new infections. In contrast, generalized immunity of the hosts determines the likelihood of clinical symptoms. Hosts are less likely to show symptoms with repeated infections but can still be re-infected by antigenically new strains and contribute to transmission. Our modeling strategy combines the advantages of both the traditional compartmental epidemiological models (i.e., tracking transmission dynamics and population immunity responses to different levels of transmission intensity) [12, 16–18] and population genetics ones (i.e., tracking within-host dynamics with detailed consideration of fitness cost and competition among strains) [25–28, 53]. With varying strain diversity, vectorial capacity, and resistance cost, we explore the key questions outlined above: whether strain diversity modulates the equilibrium resistance frequency given different transmission intensities, as well as changes in this frequency after drug withdraw, and whether the model explains the biogeographic patterns of drug resistance evolution. We then verify the main qualitative outcome from the model against the empirical biogeographic patterns of chloroquine resistance evolution.

Results

Model structure

In the compartmental ODE model, hosts' strain-specific immunity (S) regulates infectivity of parasite strains, while generalized immunity (G) determines symptomatic rate (Fig. 1; see model details in Material and Methods and S1 Appendix). Hosts are tracked in different classes of generalized immunity (G) and drug usage status (untreated, U; treated, D). Hosts move to a higher G class if they have cleared enough infections and go back to a lower class if they lose generalized immunity (Fig. 1B; $G_i \rightarrow G_j$, S1A Fig). Lower G classes correspond to more severe and apparent symptoms, which increase the likelihood of being treated by drugs ($U \rightarrow D$). The population sizes of resistant (PR) or sensitive (wild-type; PW) parasites are tracked separately in host compartments of different G and drug status. Since hosts can harbor multiple parasite strains, parasites are assumed to be distributed independently and randomly among hosts within the same compartment ([54]). Parasites can move between the compartments via the movement of hosts that harbor them, or can be added to or subtracted from the compartments via new infections and parasite clearance respectively. PW can be cleared by host immunity and drug-treatment, while

PR can only be cleared by host immunity. However, PR has a cost, s, in transmissibility, and the cost is higher in mixed-genotype (s_{mixed}) infections than in single-genotype infections (s_{single}) following [24, 52, 55].

Instead of tracking antigenic diversity explicitly, we assume parasites have $n_{strains}$ with unique antigen compositions at the population level. We incorporate specific immunity by calculating the probability of seeing a new strain given a G class upon being bitten by an infectious mosquito,

$$\eta_i = (1 - \frac{1}{n_{strains}})^{\nu_i} \tag{1}$$

where ν_i is the average number of cumulative infections received and cleared by a host in class G_i.

Non-linear relationship between vectorial capacity and prevalence

The equilibrium prevalence of wild-type-only transmissions was explored across the empirical range of antigenic strain diversity and vectorial capacity observed in the field. Specifically, the number of unique strains ranges from 6 to 447, which corresponds to a pool of 360 to 27,000 unique surface antigens [30, 31]. Mosquito bites follow a sinusoidal curve (S1 Appendix), representing a peak transmission period in the wet season, and low transmission in the dry season annually, with a mean vectorial capacity from 0.007 to 5.8. This range encompasses the lowest vectorial capacity to maintain a constant transmission to the level of high transmission settings in Africa [56]. Within the parameter ranges, prevalence peaked at an intermediate vectorial capacity given a specific strain diversity, except for the highest diversity (Fig. 2A, S2 Fig). Given the same diversity, the hump-shaped pattern of prevalence and vectorial capacity was also observed in earlier models where superinfection is allowed and immunity strengthens with prior exposures [36, 57]. This is mainly due to the fact that as vectorial capacity increases, although transmission becomes much more frequent, infectivity of a new bite per G class quickly decreases as hosts are exposed to the same strains (S3 Fig).

Drug-resistance and disease prevalence

Interestingly, the frequency of resistance decreases with increasing parasite prevalence, regardless of the specific combinations of vectorial capacity and strain diversity (Fig. 2B,C; S4 Fig). The fitness costs of single- and mixed-genotype infections only influence the slope of the relationship and the range of coexistence of resistant and wild-type parasites, but do not alter the negative relationship qualitatively (Fig. 2C; S4 Fig). Therefore, in the following sections, we only present results from one set of fitness cost combinations (i.e., $s_{single} = 0.1$ and $s_{mixed} = 0.9$ to be consistent with an earlier modeling study of parasite competition [24]).

The negative relationship between resistance and prevalence is corroborated by the empirical observation of the chloroquine-resistant genotype. The global trend of the critical chloroquine-resistant mutation *pfcrt* 76T follows an overall decline in frequency with increasing prevalence, which qualitatively agrees with the similar relationship from our model (Fig 3; beta regression, p-value$< 2e-16$). Samples from Asia and South America cluster around low prevalence and high resistance regions, whilst samples from Oceania and Africa display a wide range of prevalence and resistance frequency.

Dynamics of resistance invasion

The pattern of drug-resistance and disease prevalence arises from the interaction between host immunity, drug treatment, and resistance invasion. In order to inspect the

dynamics of resistance invasion in detail, we select a subset of strain diversity and vectorial capacity combinations as representative scenarios for the empirical gradient of low to high transmission settings for the following analyses (white squares in Fig. 2 A). So far, we have assumed that strain diversity and vectorial capacity may vary independently. However, in empirical settings, strain diversity is the outcome of long-term coevolution between parasite transmission and host immunity, whereby high transmission regions usually correspond to high antigenic diversity and low transmission regions exhibit low antigenic diversity [30]. Therefore, given the level of strain diversity, we picked the vectorial capacity that generates the highest prevalence. From low to high diversity/transmission, hosts' generalized immunity increases accordingly (higher fraction of hosts in G_1 or G_2 classes in Fig. 4). When drug treatments are applied in a wild-type only transmission setting, parasite prevalence is significantly reduced (S2 Fig), as is host generalized immunity (Fig. 4A upper panel). A much larger proportion of hosts stay in G_0 and G_1 when effective drug treatment is applied compared to when there is no treatment. In addition, the proportion of hosts in drug-treated status increases under higher diversity. If instead, the resistant genotype is present in the parasite population and starts invading when the drug is applied, hosts' generalized immunity is comparable at equilibrium to that of the no-treatment scenario (Fig. 4 lower panel). The drug-treated hosts in G_0 and G_1 are comparable from low to high transmission, while the frequency of resistance decreases with increasing diversity (Fig. 4 lower panel).

Temporal trajectories of resistance invasion show that parasite population size surges as resistant parasites quickly multiply (Fig. 5). In the meantime, resistance invasion boosts host immunity to a similar level before drug treatment (Fig. 5 upper panel). The surge in host immunity, in turn, reduces the advantage of resistant parasites, leading to a quick drop in parasite prevalence. Under a low diversity scenario, wild-type parasites quickly go extinct (Fig. 5A). Under high diversity, however, a high proportion of hosts in the largely asymptomatic G_2 creates a niche for wild-type parasites, because the higher transmissibility of wild-type parasites compensates for their high clearance rate under drug treatment (Fig. 5B). To summarize, the coexistence between wild-type and resistant genotypes in high diversity/transmission regions reflects an interplay between the self-limiting resistant invasion and higher transmissibility of wild-type parasites as resistant invasion elevates the overall host immunity and thus the presence of a large fraction of hosts carrying asymptomatic infections.

Response to drug policy change

In our model, low diversity scenarios suffer the slowest decline in resistant genotypes after switching to different drugs. In contrast, resistance frequency plunges quickly in high-diversity regions when the drug policy change. (Fig. 6; S5 Fig). This pattern corroborates similar observations across different biogeographic areas: while the transition of the first-line drug to ACT in Africa, such as Ghana and Kenya, resulted in a fast reduction in resistant genotypes, the reduction was only minor in Oceania, and resistant genotypes are still maintained at almost fixation in Southeast Asia and South America despite the change in the first-line drugs occurring more than 30 years ago (Fig. 7).

Comparison to a generalized-immunity-only model

Previous results demonstrate how transmission and antigenic diversity influence host immunity and hence the infectivity and symptomatic ratio, which determine the invasion success and maintenance of resistant genotypes. In order to confirm whether antigenic diversity is required to generate these patterns, we investigated a

generalized-immunity-only model, in which infectivity of a new infection per G class is set at a fixed value (i.e., taken as the mean value per G class from the full model across different scenarios; see Material and Methods). We observe a valley phenomenon (i.e., resistance frequency is both high at the two ends of prevalence; S6 Fig), which is qualitatively similar to Artzy-Randrup et al. [18]. When we compare how the host and parasite fraction in G classes change with increasing vectorial capacity, we find that because the infectivity of bites does not decrease as transmission increases, the number of drug-treated hosts keep increasing in the $G2$ class, resulting in the rising advantage of resistant genotypes (S7 Fig). The comparison between the full model versus the generalized-immunity-only one emphasizes the importance of incorporating antigenic diversity to generate a negative relationship between resistance and prevalence.

Discussion

In this paper, we present a theoretical argument, built on the basis of a mechanistic model, as to why different biogeographic regions show variation in the invasion and maintenance of antimalarial drug resistance. While past models have examined the frequency of drug resistance as a consequence of transmission intensity and generalized immunity, these models, unlike ours, failed to reproduce the observed equilibrium patterns of both a non-monotonic relationship between vectorial capacity and prevalence, and a resultant monotonic decreasing trend of resistance frequency with prevalence. This contrast stems from two main innovations of our model. First, its formulation directly links selection pressure from drug usage with local transmission dynamics through the interaction between strain-specific immunity, generalized immunity, and host immune response. Second, this formulation relies on a macroparasitic modeling structure suitable for diseases with high variation in co-occurring infections and strain diversities [54]. Hosts are not tracked as infected or susceptible; rather, the distribution of infections in hosts of different immunity classes is followed so that within-host dynamics of parasites can be easily incorporated.

In essence, the dynamics of resistant genotypes of a single locus are governed by two opposing forces: the selective advantage from drug usage and the cost of resistance. Both forces emerge however from local transmission dynamics, contrary to many earlier population genetics or epidemiological models that set these as fixed parameters. For example, when a fixed fraction of hosts is assumed to be drug-treated upon infection (e.g., in [12, 26–28]), the frequency of resistance is found to be unrelated to transmission intensity or requires other mechanisms to explain why resistance is prevalent in low transmission regions. Later models recognize the importance of clinical immunity gained through repeated reinfections (analogous to the $G2$ class in our model), in reducing drug usage [16, 18]. However, in these models, the infectivity of new bites of each immunity class is still fixed regardless of the transmission dynamics. Under high transmission, the clinically immune class still receives numerous new infections, and the lowered symptomatic rate does not offset the amount of drug treatment, giving rise to the increasing resistance prevalence at the high end of vectorial capacity (see S6 Fig and [18]). In contrast, in our model the selective pressure from drug treatment not only depends on the host ratio in the clinically immune class, but also on the infectivity of new bites regulated by specific immune memory. Therefore, when the host population suffers a high parasite prevalence, most hosts have experienced many infections and have entered the clinically immune class, where the drastically reduced infectivity coupled with the reduced symptomatic rate result in an overall reduced drug treatment per infection, mitigating the advantage of resistance.

Cost of resistance in terms of its form and strength is a complicated topic by itself. On the one hand, replication rates of resistant parasites are consistently found to be

slower such that they produce less parasitemia during the infection than wild-type parasites [52, 58, 59]. On the other hand, field studies also show that the transmissibility could be partially compensated by a higher gametocyte production (reviewed in [60]). Here we assume resistant parasites have lower transmissibility, but the cost differs between mixed- vs. single-genotype infections. Empirical and modeling studies [24, 51, 52] have shown that within-host competition between resistant and wild-type infections results in a higher cost for resistant infections than in single genotype infections. This phenomenon could potentially prevent resistance establishment under high-transmission settings where mixed-genotype infections are more common [24]. However, we did not find that the higher cost in mixed-genotype infections influenced the qualitative pattern of a negative relationship between transmission intensity (represented by parasite prevalence) and resistance frequency. In addition, an equal cost in mixed- vs. single-genotype infections also produced a lower frequency of resistance at high-transmission in the full model, but not in the GI-only model, indicating that within-host competition will exacerbate the disadvantage of resistant parasites under high-transmission, but does not generate the negative correlation. The temporal dynamics of resistance invasion showed that the self-limiting property of resistant parasites creates a specific niche for wild-type infections to coexist. Specifically, as resistance invades, hosts experience more infections, leading to higher generalized immunity. Wild-type infections will then dominate in the lower symptomatic class because they have higher transmissibility.

The inclusion of strain diversity in the model provides a new mechanistic explanation as to why Southeast Asia has been the original source of resistance to certain antimalarial drugs, including chloroquine. In these regions with low strain diversity, parasites cannot repeatedly re-infect hosts. Therefore, clinically immune hosts do not carry infections very often. Thus, in our model resistant strains reach fixation or near-fixation regardless of the actual vectorial capacity, and upon removal of the drug pressure, these regions continue to maintain high levels of drug resistance for a prolonged time. In contrast, high-diversity regions (e.g. Africa) should show a wide range of resistance frequency depending on how antigenic diversity is matched with local vectorial capacities, and should respond more rapidly to changing drug pressures. These results are partially corroborated by a comparison with regions that have higher transmission than Southeast Asia but low diversity (e.g. Papua New Guinea) [30]. The resistance trends for Papua New Guinea behave most similarly to those for Southeast Asia, suggesting that strain diversity, instead of vectorial capacity, is key to predicting trends in drug-resistance frequency.

Comprehensive as the model is, it still has some limitations. First, it currently assumes that resistance is determined by a single locus. If resistance needs to be encoded by two or more loci, past population genetic models demonstrate that rates of recombination could strongly influence the spread and maintenance of resistance [25, 27]. However, as recombination is one of the potential reasons explaining why multilocus resistance has delayed appearance in high-transmission regions, the incorporation of recombination is not expected to alter the negative relationship between resistance and prevalence. These earlier population genetics models of drug resistance posit that a high selfing rate in low transmission ensures high linkage among multilocus resistance, promoting their higher frequencies [27, 29, 61]. It is thus expected that adding multilocus resistance will augment the negative correlation between resistance and prevalence. Expansion of the current model to include multilocus resistance will shed light on this prediction.

The second potential limitation of our model lies in the assumption that parasites are independently and randomly distributed in hosts, while the negative binomial distribution (NBD) is widely used in macroparasitic models [54]. Empirical evidence of

parasite burdens is usually over-dispersed in that relatively few members of the host population harbor the majority of the parasite population [62–64]. In our model, we argue that despite the MOI within each G class being Poisson distributed, the population-level MOI distribution is over-dispersed as hosts in the $G2$ class are much less likely to be infected than in $G1$ or $G0$ (S3 Fig) and hosts in drug-treated classes have lower MOI than untreated classes as they harbor mostly resistant parasites only. By discretization of host classes and parasite types, we considered over-dispersion at the population level. Future models could expand on the NBD for individual classes by fitting empirical data from different age classes.

Lastly, our model assumed a random association between resistant genotype and antigenic diversity. In reality, in the early stage of invasion, the resistant genotype should have a limited antigenic background until it becomes widespread. In an agent-based stochastic model, Whitlock et al. [19] found that selection for high antigenic variation in high transmission slows the spread of resistance. The interference of immune selection and resistance might serve as an additional reason why resistant parasites are at lower frequencies in high-transmission settings. Future stochastic models are desirable for quantifying the dynamics of interactions between antigenic variation and resistant loci under different epidemiological settings.

In sum, we show that strain diversity and associated strain-specific host immunity, dynamically tracked through the macroparasitic structure, can explain the complex relationship between transmission intensity and drug-resistance frequencies, as observed for the chloroquine resistance frequencies across different localities. Our model implies that control protocols should vary from region to region and that there is no one-size-fits-all cure for malaria control worldwide [65]. In regions of low prevalence, such as Southeast Asia, long-term goals for malaria prevention will likely not be aided by intensive drug treatment [66, 67]. In these regions, elimination of falciparum malaria through vector control measures could proceed with little effect on drug resistance levels, whereas continual drug treatment will almost certainly cause fixation or near-fixation of resistance for a prolonged period of time, even after discontinuation of one drug. In contrast, in high prevalence regions such as sub-Saharan Africa, measures of prompt switching between first-line drugs and combination therapies will be quite robust against rapid increases and prolonged maintenance of drug resistance [68].

Material and Methods

Transmission dynamics

Rather than following the infected vector populations, vectorial capacity is given by a fixed contact rate, which represents the contact rate per host at which a mosquito bites a donor host and transmits to a recipient host. This contact rate is uniform across all host classes. Hosts may harbor 0 to n_{max} strains of parasites. Those with $MOI > 1$ will be able to infect mosquitoes. However, a strain from the donor does not guarantee its successful infection in a recipient. Instead, the infections will not result if the host has reached its carrying capacity of n_{max} strains, at which they cannot harbor more infections, or if the host has encountered and acquired the specific immunity to the strain (Fig. 1A). In these cases, the MOI in the host remains constant. Otherwise, infection will result and MOI is increased by 1.

Calculating Multiplicity of Infection (MOI) and Parasite Prevalence

A major assumption that links host and parasite populations is that the number of infections in an individual host (i.e., MOI) at any time follows some pre-specified distribution. To reduce the number of parameters and simplify the model, a Poisson distribution was used for MOI within a given G and treatment class. This assumption allows us to directly calculate the prevalence (i.e. the fraction of individuals carrying at least one infection) in a given G class $i = 0, 1, 2$ and treatment class $j = U, D$ as

$$I_{i,j} = 1 - \exp(-r_{i,j}) \tag{2}$$

where r is the mean MOI of the class and is equal to

$$r_{i,j} = \frac{PW_{i,j} + PR_{i,j}}{H_{i,j}} \tag{3}$$

Above, $PW_{i,j}$ and $PR_{i,j}$ are the numbers of wild-type (W) and resistant (R) infections circulating in the host class at a given time, and are determined from the system of mechanistic differential equations (S1 Fig B). $H_{i,j}$ is the number of hosts in the class at a given time and is similarly determined by the ODE system (S1 Fig A).

One justification for using a Poisson distribution for MOI is a reduction in complexity given a lack of knowledge from empirical data; however, the model can be extended to include an implicit clustering if the Poisson distribution is replaced by a negative binomial distribution.

Finally, the population-level prevalence is thus the summation of prevalence in individual host classes,

$$I = \sum_{i,j} I_{i,j} \times (H_{i,j} / \sum H_{i,j}) \tag{4}$$

MOI Dependent Versus MOI Independent Rates

The macroparasite modeling approach also impacts how transition rates are calculated, which is different from typical SIR models. Some transition rates of host classes in the ODE system are dependent on the number of parasite infections (i.e., MOI), whereas some are independent of MOI. For example, host natural death rate ($H_{ij}\alpha$) is MOI-independent because the rate itself need not be weighted by an additional factor related to MOI. Accordingly, parasite death rate due to host natural death is $(PW_{ij} + PR_{ij})\alpha$. Alternatively, host drug treatment rate depends on MOI. The value of this rate is explicitly equal to

$$(G_{i,U} \to G_{i,D}) = H_{i,U}(t) \sum_{k=1|i,U}^{\infty} k \cdot p(k) d \tag{5}$$

where each k is the number of infections in a given host, $p(k)$ is the fraction of hosts having k infections, and d is the fixed treatment rate upon experiencing symptoms. The reason the second term is necessary is to count each separate infection as a different chance to experience symptoms. Given that this term is equal to $r_{i,U} = \frac{PW_{i,U}(t)+PR_{i,U}(t)}{H_{i,U}(t)}$, we get that

$$(G_{i,U} \to G_{i,D}) = (PW_{i,U}(t) + PR_{i,U}(t))d \tag{6}$$

Thus, the movement rates for parasites from untreated classes to drug-treated classes need to consider the host movement rates as well as the number of parasites that are "carried" by the hosts. Using resistant parasites as an example,

$$
\begin{aligned}
(PR_{i,U} \rightarrow PR_{i,D}) &= H_{i,U}(t) \sum_{k=1|i,U}^{\infty} k \cdot d \cdot k \cdot p(k) \\
&= H_{i,U}(t) E(k^2) d
\end{aligned} \tag{7}
$$

where $E(k^2)$ refers to the expectation value of the square of the MOI distribution. Given that this expectation value can be written as $var(k) + (E(k))^2$, given the Poisson assumption (which implies that $var(k)$ and $E(k)$ are equal), we finally get an overall rate of

$$
(PR_{i,U} \rightarrow PR_{i,D}) = PR_{i,U}(t)(1 + r_{i,U}^{PR})d \tag{8}
$$

where $r_{i,U}^{PR}$ is the mean MOI ($E(k)$) of resistant parasites in the $G_{i,U}$ class.

Cost of Resistance and Contributions of Wild-type and Resistant Parasites to Transmission

Also calculated using Poisson statistics are the contributions of the two parasite genotypes to transmission originating from a host in a given G class. These contributions are dependent on two fixed cost parameters - the fitness cost to transmission associated with resistance in the absence of sensitive parasites (s_{single}, for single-genotype), and the fitness cost to transmission associated with resistance due to competition with wild-type parasites present in the same host (s_{mixed}, for mixed-genotype). Parasite density is assumed to be regulated by similar resources within a host (e.g., red blood cells) regardless of MOI. Thus, each strain has a reduced transmissibility when MOI > 1. For wild-type-only infections of MOI$= k$, each strain has a transmissibility of $1/k$; for resistant-only infections, each strain has a transmissibility of $1/k \cdot (1 - s_{single})$; for mixed-genotype infections, if there are m wild-type strains and n resistant strains, transmission from n resistant strains is $\frac{n}{m+n}(1 - s_{mixed})$, while transmission from m wild-type strains is $\frac{m}{m+n} + \frac{n}{m+n} s_{mixed}$ assuming wild-type strains out-compete resistant strains in growth rates and reach a higher cumulative density during the infective period.

Based on these assumptions, we then calculate transmissibility contributions at the population level from wild-type strains in purely wild-type infections ($\phi_{WS,ij}$), wild-type strains in mixed-genotype infections ($\phi_{WM,ij}$), resistant strains in purely resistant infections ($\phi_{RS,ij}$), and resistant strains in mixed-genotype infections ($\phi_{RM,ij}$). Details on how these terms were calculated using Poisson statistics appear in the S1 Appendix. The total contributions to transmissibility from resistant and sensitive parasites at a given time step are then

$$
\Omega_{W,ij} = \phi_{WS,ij} + \phi_{WM,ij} + (\phi_{RM,ij})(s_{mixed}) \tag{9}
$$

$$
\Omega_{R,ij} = (\phi_{RS,ij})(1 - s_{single}) + (\phi_{RM,ij})(1 - s_{mixed}) \tag{10}
$$

These contributions can then be used to determine the realized transmission rates given a vectorial capacity, as shown in the S1 Appendix.

Describing the Process of Immunity Loss

A significant challenge in developing the model is to describe a function for immunity loss for a given class. We adopted the classic equations for the dynamics of acquired

immunity boosted by exposure to infection (Eq. 2.5 from [36]). This gives the following immunity loss rate from a higher generalized immunity class to a lower one:

$$(G_{i,j} \to G_{i-1,j}) = h_{i,j} \frac{\exp(-\frac{h_{i,j}}{\Lambda})}{1 - \exp(-\frac{h_{i,j}}{\Lambda})} \tag{11}$$

In this case, $h_{i,j}$ is the sum of the inoculation rate and host death rate for the $G_{i,j}$ class and is determined mechanistically, and Λ is a fixed immunity loss rate parameter with dimensions of $1/[time]$. The second factor in the equation represents the failure of boosting, i.e., the probability that an individual is infected after the period of immunity has ended given that they were not infected within the immune state [69].

Empirical database and Regression Analysis

We acquired resistance marker *pfcrt* 76T frequencies from the Worldwide Antimalarial Resistance Network(WWARN). The website obtained resistant frequencies from 587 studies between 2001 and 2022 with specific curation methodologies. We then extracted geographic sampling locations from the database, and extracted *Pf* prevalence data estimated from 2-10 years old children from Malaria Atlas Project. The Malaria Atlas Project does not have predicted prevalence before 2000, while the change in first-line antimalarial drugs started around early 2000 in most African countries. We therefore restricted our empirical comparisons of equilibrium levels of resistance and prevalence to studies that conducted surveys between 1990 and 2000 and used estimated prevalence from the year 2000 as the proxy for this sampling period. Studies with a host sampling size of less than 20 were excluded. Data sources on drug usage and policies for different countries are summarized in Table1.

The relationship between prevalence and resistant frequency was investigated using beta regression because both the explanatory variable and response variable are proportions, restricted to the unit interval (0,1) [70, 71]. Thus, the proper distribution of the response variable (here, resistant prevalence) should be a beta distribution with a mean and precision parameter. Since resistant frequency also has extremes of 0 and 1, we transformed the frequency data to restrict its range between 0 and 1 first so that beta regression still applies,

$$freq_{adj} = (freq \cdot (n-1) + 0.5)/n \tag{12}$$

where n is the sample size [72]. We then used *betareg* function from R package *betareg* to perform the regression [73].

Table 1. Source of drug policy data.

Country	Citations
Kenya	[10]
Ghana	[68]
Cambodia	[66]
Thailand	[65, 66]
Papua New Guinea	[74]
Brazil	[75]

Supporting information

S1 Fig. Compartment model of drug resistance evolution. (A) The number of hosts and movements are tracked in different generalized immunity classes (G),

together with their drug treatment states (treated, D; untreated, U); **(B)** wild-type (PW) and resistant parasite (PR) population sizes are tracked in different host immunity classes; **(C)** Changes in total immunity (TI, total number of cleared infections) per G class are followed. See S1 Appendix for a detailed explanation of the ODE system.

S2 Fig. Prevalence given the combination of vectorial capacity and the number of strains from no treatment to high treatment rate. Grey areas indicate that transmission is eliminated.

S3 Fig. Infectivity of a new infection as a function of the number of strains and mean immunity (Total immunity divided by the number of hosts per G class) (see Eq. 1).

S4 Fig. Relationship between parasite prevalence and resistance frequency. Each subgraph represents the combination of resistance fitness costs in hosts with resistant strains alone (s_{single}) or mixed-genotype infections of resistant and wild-type strains (s_{mixed}).

S5 Fig. Percentage of reduction in resistance after one year of policy change in drug treatment as a function of vectorial capacity and the number of strains.

S6 Fig. Relationship between parasite prevalence and resistance frequency for the generalized-immunity-only model. Paths are connected from low vectorial capacity to high vectorial capacity. Colors represent different combinations of single-genotype infection cost and mixed-genotype infection cost of resistant parasites.

S7 Fig. Relationship between host immunity, drug treatment, and resistance evolution for the generalized-immunity-only model. Note that in the generalized-immunity-only model, there is no strain diversity. The only parameter that determines transmission intensity is vectorial capacity. In general, prevalence (blue dotted line) increases as vectorial capacity increases despite hosts increasingly concentrating in G_2 class **(A)**. The fraction of resistant parasites decreases initially with increasing vectorial capacity, but rises again as high transmission results in a higher proportion of G_2 hosts in the drug-treated class **(B)**.

S1 Appendix. The full compartmental ODE model description.

S1 Table. Epidemiological parameters used for numerically solving ODEs.

Acknowledgments

We thank Mercedes Pascual for valuable suggestions on earlier versions of the model, and Karen Day and Kathryn Tiedje for their helpful discussions and feedback related to this work. We appreciate the support of Information Technology at Purdue University through the computational resources of the Bell Community Cluster.

References

1. zur Wiesch PA, Kouyos R, Engelstädter J, Regoes RR, Bonhoeffer S. Population biological principles of drug-resistance evolution in infectious diseases. The Lancet Infectious Diseases. 2011;11(3):236–247. doi:10.1016/S1473-3099(10)70264-4.

2. Blasco B, Leroy D, Fidock DA. Antimalarial drug resistance: linking Plasmodium falciparum parasite biology to the clinic. Nature Medicine. 2017;23(8):917–928. doi:10.1038/nm.4381.

3. Ecker A, Lehane AM, Clain J, Fidock DA. PfCRT and its role in antimalarial drug resistance. Trends in Parasitology. 2012;28(11):504–514. doi:https://doi.org/10.1016/j.pt.2012.08.002.

4. Dondorp AM, Nosten F, Yi P, Das D, Phyo AP, Tarning J, et al. Artemisinin Resistance in Plasmodium falciparum Malaria. New England Journal of Medicine. 2009;361(5):455–467. doi:10.1056/NEJMoa0808859.

5. Noedl H, Se Y, Schaecher K, Smith BL, Socheat D, Fukuda MM. Evidence of Artemisinin-Resistant Malaria in Western Cambodia. New England Journal of Medicine. 2008;359(24):2619–2620. doi:10.1056/NEJMc0805011.

6. Chaijaroenkul W, Ward SA, Mungthin M, Johnson D, Owen A, Bray PG, et al. Sequence and gene expression of chloroquine resistance transporter (pfcrt) in the association of in vitro drugs resistance of Plasmodium falciparum. Malaria Journal. 2011;10(1):42. doi:10.1186/1475-2875-10-42.

7. Best Plummer W, Pinto Pereira LM, Carrington CVF. Pfcrt and pfmdr1 alleles associated with chloroquine resistance in Plasmodium falciparum from Guyana, South America. Memorias Do Instituto Oswaldo Cruz. 2004;99(4):389–392. doi:10.1590/s0074-02762004000400008.

8. Talisuna AO, Langi P, Bakyaita N, Egwang T, Mutabingwa TK, Watkins W, et al. Intensity of malaria transmission, antimalarial-drug use and resistance in Uganda: what is the relationship between these three factors? Transactions of the Royal Society of Tropical Medicine and Hygiene. 2002;96(3):310–317. doi:10.1016/S0035-9203(02)90108-2.

9. Narh CA, Ghansah A, Duffy MF, Ruybal-Pesántez S, Onwona CO, Oduro AR, et al. Evolution of Antimalarial Drug Resistance Markers in the Reservoir of Plasmodium falciparum Infections in the Upper East Region of Ghana. The Journal of Infectious Diseases. 2020;222(10):1692–1701. doi:10.1093/infdis/jiaa286.

10. Hemming-Schroeder E, Umukoro E, Lo E, Fung B, Tomás-Domingo P, Zhou G, et al. Impacts of Antimalarial Drugs on Plasmodium falciparum Drug Resistance Markers, Western Kenya, 2003–2015. The American Journal of Tropical Medicine and Hygiene. 2018;98(3):692–699. doi:10.4269/ajtmh.17-0763.

11. Lanteri CA, Chaorattanakawee S, Lon C, Saunders DL, Rutvisuttinunt W, Yingyuen K, et al. Ex Vivo Activity of Endoperoxide Antimalarials, Including Artemisone and Arterolane, against Multidrug-Resistant Plasmodium falciparum Isolates from Cambodia. Antimicrobial Agents and Chemotherapy. 2014;58(10):5831–5840. doi:10.1128/AAC.02462-14.

12. Koella J, Antia R. Epidemiological models for the spread of anti-malarial resistance. Malaria Journal. 2003;2(1):3. doi:10.1186/1475-2875-2-3.

13. Diallo D, Sutherland C, Nebie I, Konaté A, Ord R, Pota H, et al. Sustained use of insecticide-treated curtains is not associated with greater circulation of drug-resistant malaria parasites, or with higher risk of treatment failure among children with uncomplicated malaria in Burkina Faso. The American journal of tropical medicine and hygiene. 2007;76:237–44. doi:10.4269/ajtmh.2007.76.237.

14. Shah M, Kariuki S, Eng JV, Blackstock AJ, Garner K, Gatei W, et al. Effect of Transmission Reduction by Insecticide-Treated Bednets (ITNs) on Antimalarial Drug Resistance in Western Kenya. PLOS ONE. 2011;6(11):e26746. doi:10.1371/journal.pone.0026746.

15. Shah M, Omosun Y, Lal A, Odero C, Gatei W, Otieno K, et al. Assessment of molecular markers for anti-malarial drug resistance after the introduction and scale-up of malaria control interventions in western Kenya. Malaria Journal. 2015;14(1):75. doi:10.1186/s12936-015-0588-4.

16. Klein EY, Smith DL, Boni MF, Laxminarayan R. Clinically immune hosts as a refuge for drug-sensitive malaria parasites. Malaria Journal. 2008;7(1):67. doi:10.1186/1475-2875-7-67.

17. Klein EY, Smith DL, Laxminarayan R, Levin S. Superinfection and the evolution of resistance to antimalarial drugs. Proceedings of the Royal Society B: Biological Sciences. 2012;279(1743):3834–3842. doi:10.1098/rspb.2012.1064.

18. Artzy-Randrup Y, Alonso D, Pascual M. Transmission Intensity and Drug Resistance in Malaria Population Dynamics: Implications for Climate Change. PLOS ONE. 2010;5(10):e13588. doi:10.1371/journal.pone.0013588.

19. Whitlock AOB, Juliano JJ, Mideo N. Immune selection suppresses the emergence of drug resistance in malaria parasites but facilitates its spread. PLOS Computational Biology. 2021;17(7):e1008577. doi:10.1371/journal.pcbi.1008577.

20. Ariey F, Robert V. The puzzling links between malaria transmission and drug resistance. Trends in Parasitology. 2003;19(4):158–160. doi:10.1016/S1471-4922(03)00054-0.

21. Alifrangis M, Lemnge MM, Rønn AM, Segeja MD, Magesa SM, Khalil IF, et al. Increasing prevalence of wildtypes in the dihydrofolate reductase gene of Plasmodium falciparum in an area with high levels of sulfadoxine/pyrimethamine resistance after introduction of treated bed nets. The American Journal of Tropical Medicine and Hygiene. 2003;69(3):238–243.

22. Mharakurwa S, Mutambu SL, Mudyiradima R, Chimbadzwa T, Chandiwana SK, Day KP. Association of house spraying with suppressed levels of drug resistance in Zimbabwe. Malaria Journal. 2004;3(1):35. doi:10.1186/1475-2875-3-35.

23. Myers-Hansen JL, Abuaku B, Oyebola MK, Mensah BA, Ahorlu C, Wilson MD, et al. Assessment of antimalarial drug resistant markers in asymptomatic Plasmodium falciparum infections after 4 years of indoor residual spraying in Northern Ghana. PLOS ONE. 2020;15(12):e0233478. doi:10.1371/journal.pone.0233478.

24. Bushman M, Antia R, Udhayakumar V, Roode JCd. Within-host competition can delay evolution of drug resistance in malaria. PLOS Biology. 2018;16(8):e2005712. doi:10.1371/journal.pbio.2005712.

25. Hastings IM. Complex dynamics and stability of resistance to antimalarial drugs. Parasitology. 2006;132(5):615–624. doi:10.1017/S0031182005009790.

26. Curtis CF, Otoo LN. A simple model of the build-up of resistance to mixtures of anti-malarial drugs. Transactions of the Royal Society of Tropical Medicine and Hygiene. 1986;80(6):889–892. doi:10.1016/0035-9203(86)90248-8.

27. Dye C, Williams BG. Multigenic drug resistance among inbred malaria parasites. Proceedings of the Royal Society of London Series B: Biological Sciences. 1997;264(1378):61–67. doi:10.1098/rspb.1997.0009.

28. Hastings IM. A model for the origins and spread of drug-resistant malaria. Parasitology. 1997;115(2):133–141. doi:10.1017/S0031182097001261.

29. Hastings IM, D'Alessandro U. Modelling a Predictable Disaster:: The Rise and Spread of Drug-resistant Malaria. Parasitology Today. 2000;16(8):340–347. doi:10.1016/S0169-4758(00)01707-5.

30. Chen DS, Barry AE, Leliwa-Sytek A, Smith TA, Peterson I, Brown SM, et al. A Molecular Epidemiological Study of var Gene Diversity to Characterize the Reservoir of Plasmodium falciparum in Humans in Africa. PLOS ONE. 2011;6(2):e16629. doi:10.1371/journal.pone.0016629.

31. Tonkin-Hill GQ, Trianty L, Noviyanti R, Nguyen HHT, Sebayang BF, Lampah DA, et al. The Plasmodium falciparum transcriptome in severe malaria reveals altered expression of genes involved in important processes including surface antigen–encoding var genes. PLOS Biology. 2018;16(3):e2004328. doi:10.1371/journal.pbio.2004328.

32. Volkman SK, Barry AE, Lyons EJ, Nielsen KM, Thomas SM, Choi M, et al. Recent Origin of Plasmodium falciparum from a Single Progenitor. Science. 2001;293(5529):482–484. doi:10.1126/science.1059878.

33. Day KP, Marsh K. Naturally acquired immunity to Plasmodium falciparum. Immunology Today. 1991;12(3):A68–A71. doi:10.1016/S0167-5699(05)80020-9.

34. Tiedje KE, Oduro AR, Agongo G, Anyorigiya T, Azongo D, Awine T, et al. Seasonal Variation in the Epidemiology of Asymptomatic Plasmodium falciparum Infections across Two Catchment Areas in Bongo District, Ghana. The American Journal of Tropical Medicine and Hygiene. 2017;97(1):199–212. doi:10.4269/ajtmh.16-0959.

35. Bonnet S, Gouagna LC, Paul RE, Safeukui I, Meunier JY, Boudin C. Estimation of malaria transmission from humans to mosquitoes in two neighbouring villages in south Cameroon: evaluation and comparison of several indices. Transactions of the Royal Society of Tropical Medicine and Hygiene. 2003;97(1):53–59. doi:10.1016/S0035-9203(03)90022-8.

36. Aron JL. Dynamics of acquired immunity boosted by exposure to infection. Mathematical Biosciences. 1983;64(2):249–259. doi:10.1016/0025-5564(83)90007-X.

37. Dietz K, Molineaux L, Thomas A. A malaria model tested in the African savannah. Bulletin of the World Health Organization. 1974;50(3-4):347–357.

38. Molineaux L, Gramiccia G, Organization WH, et al. The Garki project: research on the epidemiology and control of malaria in the Sudan savanna of West Africa. World Health Organization; 1980.

39. Bull PC, Lowe BS, Kortok M, Marsh K. Antibody Recognition of Plasmodium falciparum Erythrocyte Surface Antigens in Kenya: Evidence for Rare and Prevalent Variants. Infection and Immunity. 1999;67(2):733–739.

40. Bull PC, Lowe BS, Kortok M, Molyneux CS, Newbold CI, Marsh K. Parasite antigens on the infected red cell surface are targets for naturally acquired immunity to malaria. Nature medicine. 1998;4(3):358–360.

41. Rask TS, Hansen DA, Theander TG, Pedersen AG, Lavstsen T. Plasmodium falciparum Erythrocyte Membrane Protein 1 Diversity in Seven Genomes – Divide and Conquer. PLOS Computational Biology. 2010;6(9):e1000933. doi:10.1371/journal.pcbi.1000933.

42. He Q, Pilosof S, Tiedje KE, Ruybal-Pesántez S, Artzy-Randrup Y, Baskerville EB, et al. Networks of genetic similarity reveal non-neutral processes shape strain structure in Plasmodium falciparum. Nature Communications. 2018;9(1):1817. doi:10.1038/s41467-018-04219-3.

43. Pilosof S, He Q, Tiedje KE, Ruybal-Pesántez S, Day KP, Pascual M. Competition for hosts modulates vast antigenic diversity to generate persistent strain structure in Plasmodium falciparum. PLOS Biology. 2019;17(6):e3000336. doi:10.1371/journal.pbio.3000336.

44. Barry AE, Trieu A, Fowkes FJI, Pablo J, Kalantari-Dehaghi M, Jasinskas A, et al. The Stability and Complexity of Antibody Responses to the Major Surface Antigen of Plasmodium falciparum Are Associated with Age in a Malaria Endemic Area. Molecular & Cellular Proteomics : MCP. 2011;10(11). doi:10.1074/mcp.M111.008326.

45. Djimdé AA, Doumbo OK, Traore O, Guindo AB, Kayentao K, Diourte Y, et al. Clearance of drug-resistant parasites as a model for protective immunity in Plasmodium falciparum malaria. The American Journal of Tropical Medicine and Hygiene. 2003;69(5):558–563.

46. Ruybal-Pesántez S, Tiedje KE, Pilosof S, Tonkin-Hill G, He Q, Rask TS, et al. Age-specific patterns of DBLα var diversity can explain why residents of high malaria transmission areas remain susceptible to Plasmodium falciparum blood stage infection throughout life. International Journal for Parasitology. 2022;doi:10.1016/j.ijpara.2021.12.001.

47. Collins WE, Jeffery GM. A retrospective examination of sporozoite-and trophozoite-induced infections with Plasmodium falciparum in patients previously infected with heterologous species of Plasmodium: effect on development of parasitologic and clinical immunity. The American journal of tropical medicine and hygiene. 1999;61(1_Supplement):36–43.

48. Nkhoma SC, Trevino SG, Gorena KM, Nair S, Khoswe S, Jett C, et al. Resolving within-host malaria parasite diversity using single-cell sequencing. bioRxiv. 2018; p. 391268. doi:10.1101/391268.

49. Wong W, Griggs AD, Daniels RF, Schaffner SF, Ndiaye D, Bei AK, et al. Genetic relatedness analysis reveals the cotransmission of genetically related Plasmodium falciparum parasites in Thiès, Senegal. Genome Medicine. 2017;9(1):1–12.

50. Henden L, Lee S, Mueller I, Barry A, Bahlo M. Identity-by-descent analyses for measuring population dynamics and selection in recombining pathogens. PLoS genetics. 2018;14(5):e1007279.

51. de Roode JC, Culleton R, Bell AS, Read AF. Competitive release of drug resistance following drug treatment of mixed Plasmodium chabaudi infections. Malaria Journal. 2004;3(1):33. doi:10.1186/1475-2875-3-33.

52. Bushman M, Morton L, Duah N, Quashie N, Abuaku B, Koram KA, et al. Within-host competition and drug resistance in the human malaria parasite Plasmodium falciparum. Proceedings of the Royal Society B: Biological Sciences. 2016;283(1826):20153038.

53. Hastings IM, Watkins WM, White NJ. The Evolution of Drug-Resistant Malaria: The Role of Drug Elimination Half-Life. Philosophical Transactions: Biological Sciences. 2002;357(1420):505–519.

54. Anderson RM, May RM. Regulation and Stability of Host-Parasite Population Interactions: I. Regulatory Processes. Journal of Animal Ecology. 1978;47(1):219–247. doi:10.2307/3933.

55. Harrington W, Mutabingwa T, Muehlenbachs A, Sorensen B, Bolla M, Fried M, et al. Competitive facilitation of drug-resistant Plasmodium falciparum malaria parasites in pregnant women who receive preventive treatment. Proceedings of the National Academy of Sciences. 2009;106(22):9027–9032.

56. Garrett-Jones C, Shidrawi G. Malaria vectorial capacity of a population of Anopheles gambiae: an exercise in epidemiological entomology. Bulletin of the World Health Organization. 1969;40(4):531.

57. Elderkin RH, Berkowitz DP, Farris FA, Gunn CF, Hickernell FJ, Kass SN, et al. On the steady state of an age-dependent model for malaria. In: Lakshmikantham V, editor. Nonlinear Systems and Applications. Academic Press; 1977. p. 491–512.

58. ETHZentrum N. Linking evolutionary ecology with epidemiology. Revue suisse de zoologie. 1994;101(4):865–874.

59. De Roode JC, Helinski ME, Anwar MA, Read AF. Dynamics of multiple infection and within-host competition in genetically diverse malaria infections. The American Naturalist. 2005;166(5):531–542.

60. Koella JC. Costs and Benefits of Resistance against Antimalarial Drugs. Parasitology Today. 1998;14(9):360–364. doi:10.1016/S0169-4758(98)01297-6.

61. Hastings IM, Donnelly MJ. The impact of antimalarial drug resistance mutations on parasite fitness, and its implications for the evolution of resistance. Drug Resistance Updates. 2005;8(1):43–50. doi:10.1016/j.drup.2005.03.003.

62. Anderson RM, Gordon DM. Processes influencing the distribution of parasite numbers within host populations with special emphasis on parasite-induced host mortalities. Parasitology. 1982;85(2):373–398. doi:10.1017/S0031182000055347.

63. Churcher T, Ferguson N, Basanez MG. Density dependence and overdispersion in the transmission of helminth parasites. Parasitology. 2005;131(1):121–132.

64. Grogan LF, Phillott AD, Scheele BC, Berger L, Cashins SD, Bell SC, et al. Endemicity of chytridiomycosis features pathogen overdispersion. Journal of Animal Ecology. 2016;85(3):806–816.

65. Rasmussen C, Alonso P, Ringwald P. Current and emerging strategies to combat antimalarial resistance. Expert Review of Anti-infective Therapy. 2022;20(3):353–372. doi:10.1080/14787210.2021.1962291.

66. Delacollette C, D'Souza C, Christophel E, Thimasarn K, Abdur R, Bell D, et al. MALARIA TRENDS AND CHALLENGES IN THE GREATER MEKONG SUBREGION. SOUTHEAST ASIAN J TROP MED PUBLIC HEALTH. 2009;40(4):19.

67. Imwong M, Dhorda M, Myo Tun K, Thu AM, Phyo AP, Proux S, et al. Molecular epidemiology of resistance to antimalarial drugs in the Greater Mekong subregion: an observational study. The Lancet Infectious Diseases. 2020;20(12):1470–1480. doi:10.1016/S1473-3099(20)30228-0.

68. Flegg JA, Metcalf CJE, Gharbi M, Venkatesan M, Shewchuk T, Hopkins Sibley C, et al. Trends in Antimalarial Drug Use in Africa. The American Journal of Tropical Medicine and Hygiene. 2013;89(5):857–865. doi:10.4269/ajtmh.13-0129.

69. Aron JL, May RM. The population dynamics of malaria. In: Anderson RM, editor. The Population Dynamics of Infectious Diseases: Theory and Applications. Boston, MA: Springer US; 1982. p. 139–179. Available from: `http://link.springer.com/10.1007/978-1-4899-2901-3_5`.

70. Ferrari S, Cribari-Neto F. Beta regression for modelling rates and proportions. Journal of applied statistics. 2004;31(7):799–815.

71. Simas AB, Barreto-Souza W, Rocha AV. Improved estimators for a general class of beta regression models. Computational Statistics & Data Analysis. 2010;54(2):348–366.

72. Smithson M, Verkuilen J. A better lemon squeezer? Maximum-likelihood regression with beta-distributed dependent variables. Psychological methods. 2006;11(1):54.

73. Cribari-Neto F, Zeileis A. Beta Regression in R. Journal of Statistical Software. 2010;34(2):1–24. doi:10.18637/jss.v034.i02.

74. Nsanzabana C, Hastings IM, Marfurt J, Muüller I, Baea K, Baea K, et al. Quantifying the evolution and impact of antimalarial drug resistance: drug use, spread of resistance, and drug failure over a 12-year period in Papua New Guinea. The Journal of infectious diseases. 2010;201(3):435–443.

75. Gama BE, de Oliveira NKA, Zalis MG, de Souza JM, Santos F, Daniel-Ribeiro CT, et al. Chloroquine and sulphadoxine-pyrimethamine sensitivity of Plasmodium falciparum parasites in a Brazilian endemic area. Malaria journal. 2009;8(1):1–5.

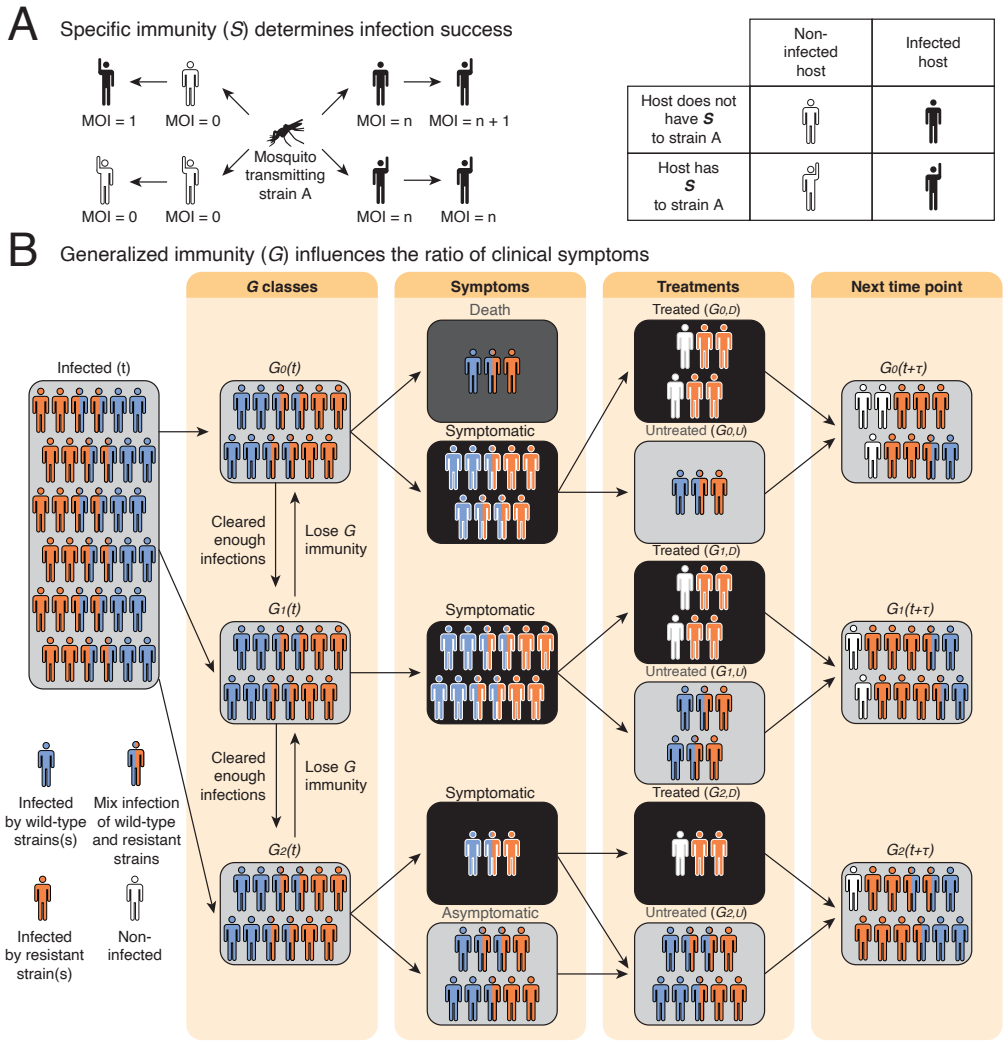

Fig 1. Schematic illustration of transmission rules and acquisition of host immunity within the compartmental ODE model (see S1 Fig for a detailed representation of the compartment model). **(A)** Rules for new infections given the host's past infection history and current multiplicity of infection (i.e., MOI). Upon transmission of a specific parasite strain A, if the host has had an infection of strain A in the past (hands raised), a new infection will not be added to the current MOI; instead, the infection will be considered cleared and added to the total number of cleared infections; if the host is new to strain A and does not have specific immunity to it (inferred from Eq. 1), a new infection will be added (i.e., MOI increase by 1) as long as MOI does not exceed the carrying capacity of coexisting strains. **(B)** Rules of symptomatic infections and treatment in the different generalized immunity (G) classes. With increasing generalized immunity (G), hosts are less likely to show clinical symptoms. Hosts in G_0 have a risk of death in addition to symptomatic infections; Hosts in G_1 do not die from infections but show symptoms upon new infections; Hosts in G_2 carry asymptomatic infections most of the time with a slight chance of showing symptoms. Symptomatic infections result in a daily treatment rate that removes the infections caused by wild-type strains. Hosts that have cleared enough number of infections will move to the next G class. Hosts will move back to a lower G class when the generalized immunity memory is slowly lost if not boosted by constant infections.

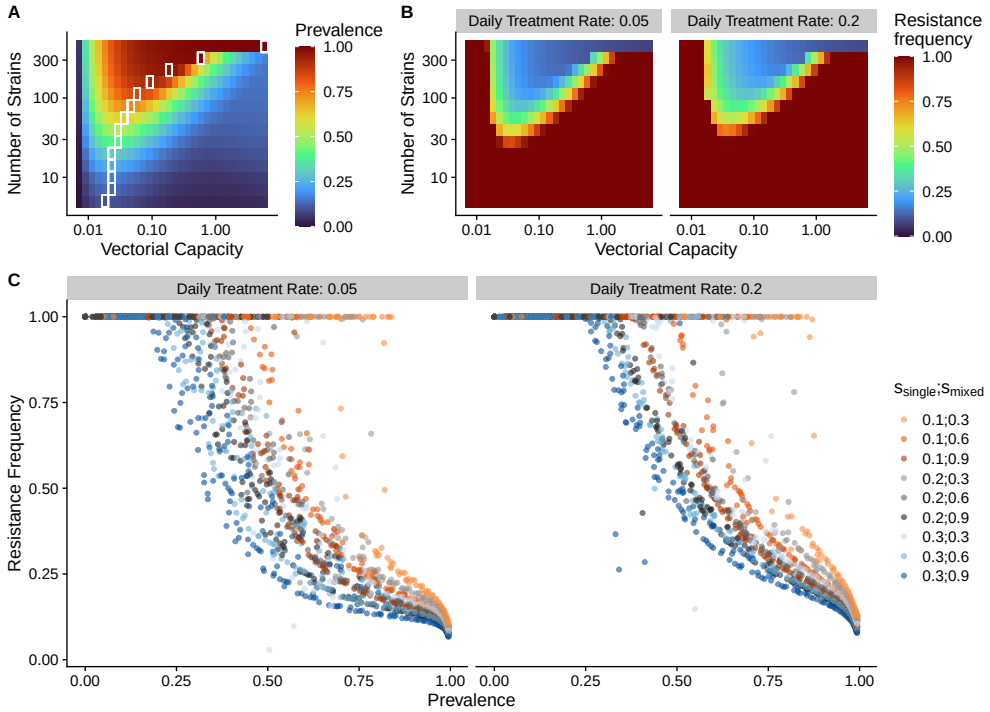

Fig 2. The frequency of resistance under varying strain diversity and vectorial capacity. (A) The heatmap shows a nonlinear parasite prevalence response given increasing vectorial capacity and the number of strains under no drug treatment, with warmer colors representing high prevalence and cooler colors representing low prevalence. X and Y axes correspond to increasing vectorial capacity and the number of strains in logarithmic scales. White tiles indicate the highest prevalence given a fixed number of strains. **(B)** The heatmaps show resistance frequencies under varying strain diversity and vectorial capacity at two levels of drug treatment rate, with warmer colors representing higher resistance frequency (in this example, clone cost = 0.1, mix cost = 0.9). **(C)** A negative relationship between parasite prevalence and resistance frequency. The color of the points indicates combinations of resistance fitness costs in hosts with resistant strains alone (s_{single}) or mixed infections of resistant and wild-type strains (s_{mixed}).

Fig 3. Global distribution of chloroquine-resistant genotype (*pfcrt* 76T) against *P. falciparum* prevalence in children between 2-10 yrs old. Sampling between 1990 and 2000 was included to ensure genotyping was performed largely before the policy switch of the first-line antimalarial drugs to ACT. Different shapes indicate samples from different continents, while shape sizes correspond to sample sizes for genotyping (see Methods for details).

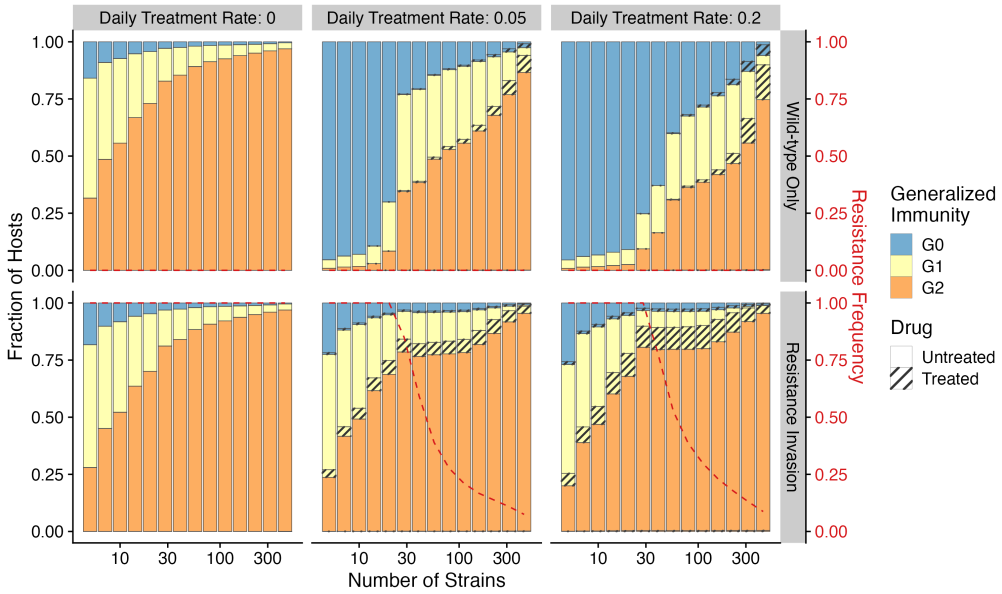

Fig 4. Relationship between host immunity, drug treatment, and resistance evolution. Fraction of hosts in different G classes with increasing strain diversity and the corresponding vectorial capacity indicated by white circles in Fig. 1A at equilibrium or year 50 after the invasion of resistant genotypes. Hosts in drug-treated classes are indicated by stripes. Red dotted lines show the corresponding frequency of resistance. The upper panel is generated under wild-type-only infections with increasing treatment rates. The lower panel represents resistance-only infections without treatment or resistant invasion under treatments.

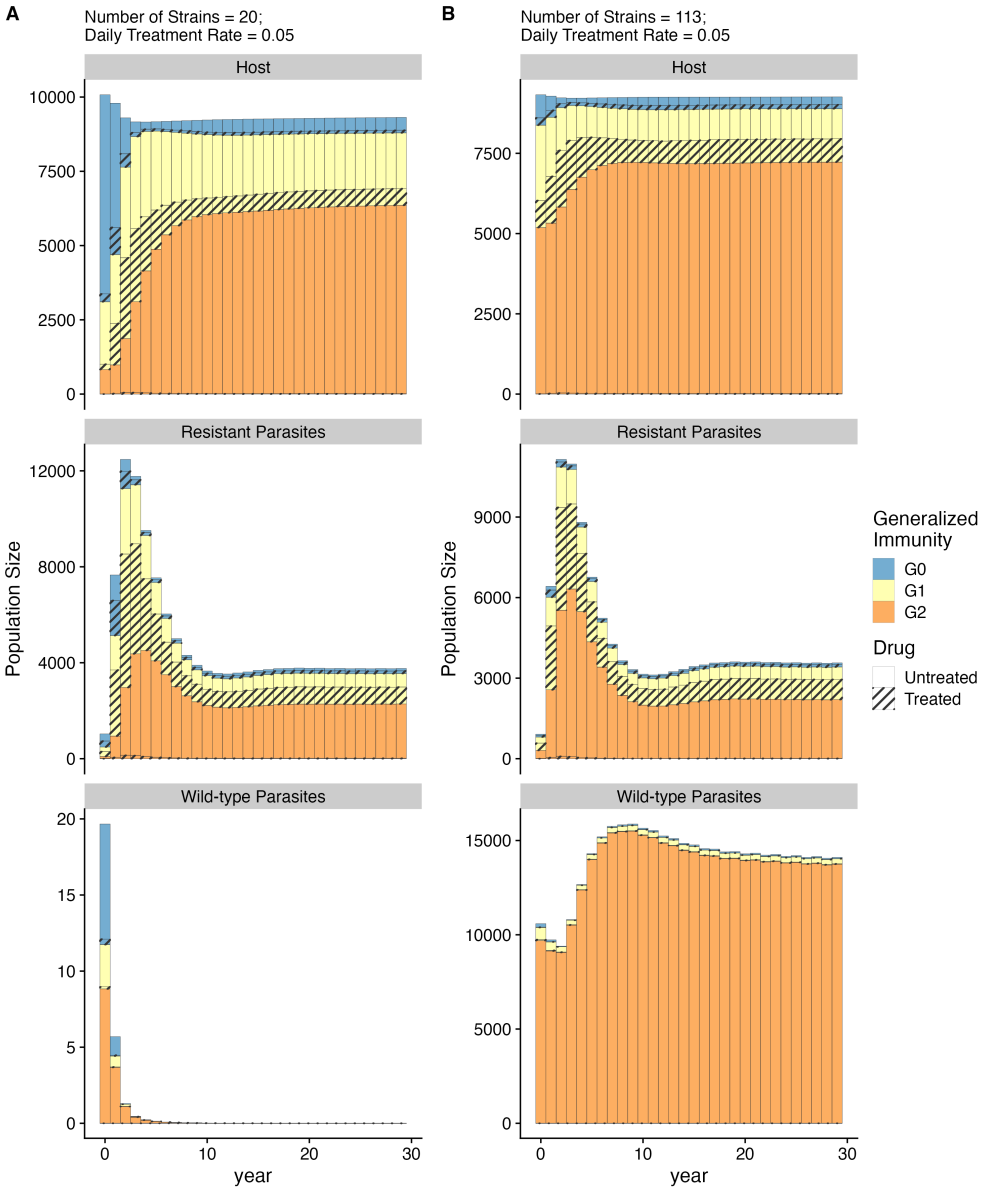

Fig 5. Temporal trajectories of resistance invasion. Host and parasite dynamics under resistance invasion are shown for lower ($n_{strains} = 20$) **A** and higher ($n_{strains} = 113$) diversity **B**. Because drug treatment does not affect resistant parasites, they surge quickly after introduction, thus leading to more infections. Hosts recovered from a large number of new infections move into higher G classes (from year 1-8). The high host immune protection selects against resistant parasites (year 4-10). Under low diversity, wild-type parasites quickly go to extinction **A**. Under high diversity, the less symptomatic G_2 class provides a niche for wild-type parasites to multiply (year 4-10), where the two genotypes co-exist. Meanwhile, resistant parasites dominate in hosts that are in G_0 and G_1 **B**.

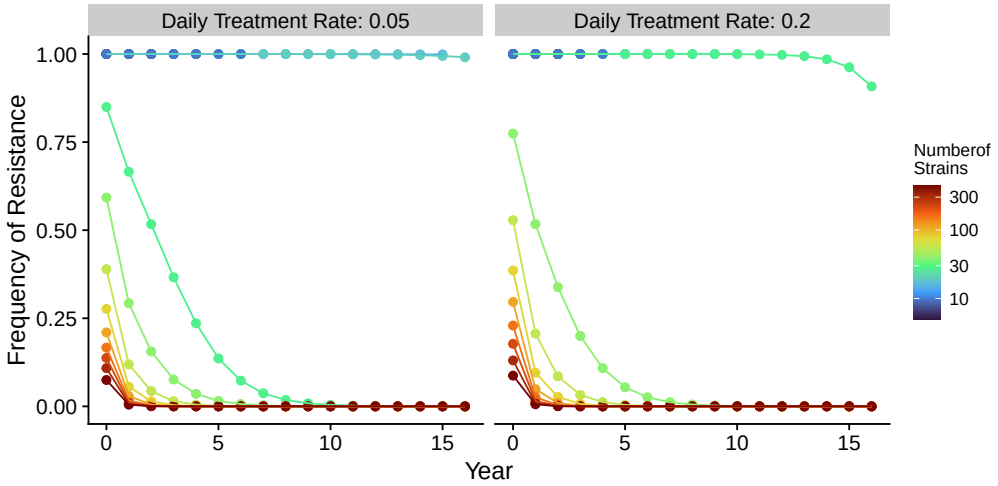

Fig 6. Changes in frequency of resistance after the first-line drug is changed. Each trajectory represents the combination of variables indicated by the white circles in Fig. 1A. Color from cool to warm represents increasing diversity in strains. Here the usage of the drug, to which parasites have developed resistance, is reduced to 0.52, 0.52, 0.52, 0.52, 0.21, 0.21, 0.21, 0.21, 0, 0, 0, 0, 0, 0, 0, 0 each year following the change in the treatment regime. The trajectory of reduction in resistant drug usage follows the usage survey in Western Kenya from 2003 to 2018 [10].

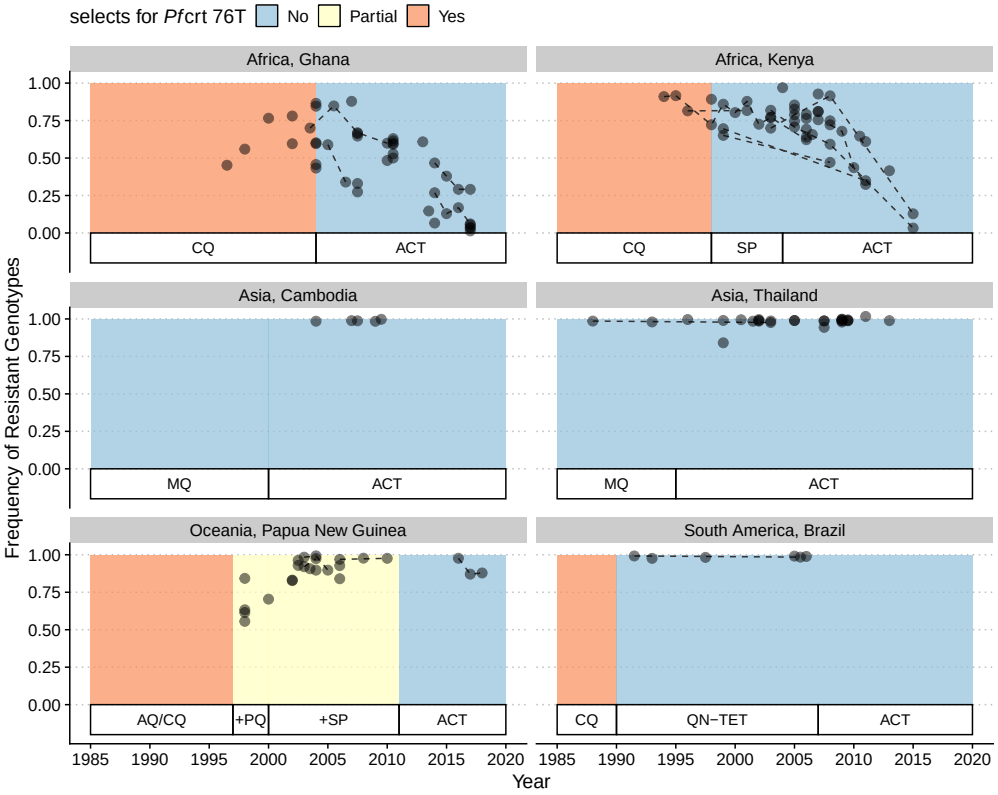

Fig 7. Changes in frequency of resistant genotypes across different biogeographic regions. Each circle represents one studied sample (at least 20 infected hosts) from one geographic location. Circles connected by dotted lines represent longitudinal samples from the same study. After the policy switch in first-line antimalarial drugs, frequencies of resistance decreased gradually in Africa, but maintained high in Asia, Oceania, and South America despite the policy change for more than 20 years. CQ: chloroquine; SP: sulfadoxine-pyrimethamine; MQ: mefloquine; AQ: amodiaquine; PQ: primaquine; QN-TET: quinine+tetracycline; ACT: artemisinin-based combination therapy.